Free Radical Research, September 2009; 43(9): 876–886

informa
healthcare

Metabolism-induced oxidative stress is a mediator of glucose toxicity in HT22 neuronal cells

LUCIA RAČKOVÁ[1,2], VLADIMÍR ŠNIRC[1], TOBIAS JUNG[2], MILAN ŠTEFEK[1], ÇIMEN KARASU[3], & TILMAN GRUNE[2]

[1]*Institute of Experimental Pharmacology and Toxicology, Slovak Academy of Sciences, Bratislava, Slovak Republic,* [2]*University Hohenheim, Institute of Biological Chemistry and Nutrition, Department of Biofunctionality and Food Safety, Stuttgart, Germany, and* [3]*Gazi University, Faculty of Medicine, Department of Medical Pharmacology, Ankara, Turkey*

(Received 17 April 2009; revised 4 June 2009)

Abstract
Oxidative stress has been widely considered as a key player in the adverse effects of hyperglycaemia to various tissues, including neuronal cells. This study examined the participation of oxidative stress in injurious effects of high glucose on HT22 cells along with the activity of proteasome, a proteolytic system responsible for degradation of oxidized proteins. Although 10-fold glucose concentration caused non-significant viability changes, a significant reduction of cell proliferation was found. Moreover, the cell morphology was also altered. These changes were followed by an enhancement of intracellular ROS generation, however without any significant boost of the carbonyl group concentration in proteins. Correspondingly, only a slight decline in the 20S proteasome activity was found in high-glucose-treated cells. On the other hand, substances affecting glucose metabolism or antioxidants partially preserved the oxidative stress in high glucose treated cells. In summary, these results highlight the role of metabolic oxidative stress in hyperglycaemia affecting neurons.

Keywords: *Metabolic oxidative stress, hyperglycaemia, diabetes, neuronal cells, proteasome, protein oxidation*

Introduction

Besides the retina, kidney and vascular tissue, neuronal tissue is one of the major targets of diabetic complications caused by chronically elevated glucose level [1]. The peripheral neuropathies [2,3] represent the most common diabetic complication triggered by the injurious effect of hyperglycaemia on neuronal cells. However, broad evidence suggests that the central nervous system is also susceptible to long-term complications associated with diabetes [4,5]. Diabetic encephalopathy is a pathology triggered by diabetes associated with morphological and functional alterations in the brain [6–10]. The central complications of hyperglycaemia also include the potentiation of neuronal damage following hypoxic/ischemic events, including stroke [4]. In diabetic animals, deficits in cognitive performance may be explained in part by the neurotoxic effects of hyperglycaemia associated with impairment of cognitive performance [11–13] and changes in glutamate neurotransmission [14].

A high production rate of reactive oxygen species (ROS) in chronic hyperglycaemia is one of the major mediators of neuronal complications in diabetes mellitus [15,16]. Several markers of oxidative stress were shown to be elevated in neurons during diabetes [16,17]. The hippocampus is particularly sensitive to oxidative stress induced by diabetes. Radioimmunocytochemistry revealed that 4-hydroxynonenal (HNE) protein conjugation, a marker of oxidative stress, is increased in all sub-regions of the hippocampus of rats suffering streptozotocin-induced diabetes [9]. Additionally, in the hippocampi of streptozotocin-treated rats, not only a strong increase in ROS is observed but also a persistent activation of NFκB [18]. Grillo et al.

Correspondence: Lucia Račková, Institute of Experimental Pharmacology and Toxicology, Slovak Academy of Sciences, Bratislava, Slovak Republic. Tel: +421-2-59410 658. Fax: +421-2-5477 5928. Email: exfadada@savba.sk

ISSN 1071-5762 print/ISSN 1029-2470 online
DOI: 10.1080/10715760903104374

[19] demonstrated that increases in oxidative stress observed in the hippocampus following hyperglycaemia may result from modulation of anti-oxidant systems, such as superoxide dismutase. Multiple biochemical pathways and mechanisms of action for glucose toxicity have been suggested [1]. All these pathways have in common the formation of reactive oxygen species, which in excess and over time can cause chronic oxidative stress. In addition, hyperglycaemia was found to cause protein glycation, which in turn might trigger oxidative stress that can contribute to further protein modification by oxidation [20,21]. Interestingly, a significant increase in protein carbonyls and HNE-protein conjugation of GLUT3 was demonstrated in hippocampi of diabetic animals [22].

In our study, we further highlighted the role of metabolic-activation-induced free-radical production and the contribution of non-enzymatic glycoxidation to the overall oxidant production in high-glucose-treated hippocampal neurons.

Materials and methods

Materials

Sigma provided anti-DNP antibodies (polyclonal rabbit). Proteasome antibodies were purchased from Biomol (Germany) (polyclonal specific for 20S sub-units). Jackson ImmunoResearch (Germany) supplied goat anti-mouse-FITC-labelled and goat anti-rabbit-TRITC-labelled antibodies. Cosmo Bio Co., Ltd (Japan) supplied anti AGE-antibodies. (±)-8-methoxy-1,3,4,4a,5,9b-hexahydro-pyrido[4,3-b]indole-2-carboxylic acid ethyl ester (AO) was synthesized at the Institute of Experimental Pharmacology SAS (Bratislava, Slovak Republic) [23,24]. All other chemicals were purchased from Sigma, Merck or Calbiochem (Germany).

Cell culture

HT22 cells (mouse hippocampal neurons) were cultured at 37°C in a 5% CO_2 atmosphere using uncoated T-75 Falcons or poly-L-lysine-coated Petri dishes (for fluorescence microscopy). Commercial high glucose DMEM cell medium, containing 10% heat-inactivated foetal bovine calf serum (FBS), 1% penicillin/streptomycin, 1% glutamine and additional 0.35% glucose was used as normal glucose (NG). The high-glucose treated HT22 cells (HG) were exposed to a 10-fold amount of glucose for 48 h. To study the effect of glycolysis inhibitors, the cells were treated with high deoxyglucose (HdG, 3.5%) medium and the HG cells were co-incubated with citrate (Cit, 3 mmol/L) and antioxidant, i.e. (±)-8-methoxy-1,3,4,4a,5,9b-hexahydro-pyrido[4,3-b]indole-2-carboxylic acid ethyl ester (AO, 0.1 mmol/L).

Viability and cell number measurements

Ten microlitres of cell suspension were added to 190 μL of trypan blue solution in PBS (0.1%) and allowed to stand for 2 min at room temperature [25]. The cells were counted in two chambers of the haematocytometer. The viability was calculated as: number of stained cells × 100/total number of cells counted = percentage of stained cells in the sample. Colourimetric assay for the quantification of cell death, based on measurement of the activity of lactate dehydrogenase (LDH) released from the cytosol of damaged cells into the supernatant, was also used to assess glucose cytotoxicity by using a kit (LDH; Roche Applied Science, Indianapolis).

Apoptosis/necrosis detection

The apoptotic changes were assessed by modified ethidium bromide and acridine orange (EtBr/AO) staining assay [26]. Briefly, the cells were grown in 6-cm collagen-coated dishes. EtBr/AO dye mix (100 μg/mL EtBr and 100 μg/mL AO, 20 μL) was added to each dish at the end of incubation in NG and HG and the cells were viewed under an Olympus BX-60 transmission fluorescence microscope running standard software. Each image was collected with excitation at 488 nm, emission at 520 nm (green). Early and late apoptotic cells were detected by their bright green or orange nucleus with condensed or fragmented chromatin, whereas necrotic cells were detected by their intact red nuclei and live cells had a green nucleus.

Proteasomal activity measurements

A volume of 10 μl cell lysate was added to the incubation buffer (450 mM Tris base; 90 mM KCl; 15 mM Mg-acetate; 15 mM $MgCl_2$ and dithiothreitol was added before the experiment to the concentration of 3 mM). The fluorogenic peptide suc-LLVY-MCA and ATP were added to the final concentration of 0.16 and 4.16 mM, respectively, to determine the ATP-dependent proteasomal activity. For determination of the ATP-independent proteasomal activity, 0.1 mg/ml hexokinase and 15 mM 2-deoxy-D-glucose were added instead of the ATP. The mixture was incubated for 30 min at 37°C. The activity was measured by cleavage of suc-LLVY-MCA. The release of the fluorochrome is directly proportional to the amount of proteolytic activity. The fluorescence was measured in a fluorimeter at an excitation wavelength of 390 and 390 nm for emission, using free MCA as standard. Since suc-LLVY-MCA is a substrate for a variety of proteases, control lysates were treated with 20 μM lactacystin, a potent proteasome inhibitor. The activities of the lactacystin-treated samples were subtracted from the respective samples showing total activity to calculate the specific proteasomal activity.

Intracellular ROS production

Cellular oxidant production in HT22 cells was determined by using a method described by Giardina and Inan [27]. The cells were seeded in 96-well plates to a density of 4×10^4/well and incubated with 15 μM H_2DCF-DA (dichlorofluorescein-diacetate) in buffer for 60 min at 37°C. H_2DCF-DA is a membrane-permeable compound which is hydrolysed by intracellular esterases resulting in formation of non-fluorescent H_2DCF (dichlorofluorescin). This compound, when oxidized by oxidants or free radicals, forms the fluorescent DCF (dichlorofluorescein) [28]. After H_2DCF-DA loading, the cells were washed with buffer and incubated in NG or HG with or without the inhibitors tested. The fluorescence of DCF was measured in a micro-plate reader fluorimeter at an excitation wavelength of 485 nm and an emission wavelength of 528 nm.

Determination of protein oxidation

Protein carbonyl measurement was performed as described by Buss et al. [29] for the assessment of protein oxidation. Samples of cell lysates were adjusted to 1 mg/ml protein, derivatized with 2,4-dinitrophenylhydrazine and adsorbed to Maxisorb multiwell plates (NUNC, Roskilde, Denmark). Protein carbonyls were detected using an anti-DNP primary antibody and an anti-rabbit-IgG peroxidase linked secondary antibody. O-Phenyl diamine was used to develop the plate and the absorbance was determined using a multi-well plate reader and a detection wavelength of 492 nm.

Immunofluorescence microscopy

Detection of protein carbonyls was performed as described previously with slight modifications [30,31]. The cells were seeded in poly-L-lysine-coated Petri dishes (50 000 cells per 3-cm dish). At the end of the incubation time in NG or HG the cells were immediately fixed for 10 min at −20°C using ethanol:ether (1:1) in order to remove cellular lipids. Afterwards, the cells were incubated for 16 h at 4°C with DNPH (300 mg DNPH per 100 ml of 96% ethanol, acidified using 1.5% of pure sulphuric acid). The primary DNP-adduct specific antibody was applied as the primary antibody, followed by labelling with the TRITC-labelled secondary antibody. For detection of proteasome distribution, a specific antibody against the 20S proteasome was used as the primary antibody and FITC-labelled goat anti-mouse as the secondary antibody. In parallel experiments an anti-AGEs monoclonal antibody (Cosmo Bio Co Ltd, Japan) was applied as the primary antibody in PBS containing 1% of foetal calf serum for 90 min at 4°C in a dilution of 2.5 μg/mL for detection of the distribution of advanced glycation end products (AGEs) following the fixation procedure. Afterwards, the cells were stained using the secondary antibody (FITC-labelled goat anti-mouse, diluted 1:100 in washing buffer) for 90 min at 4°C.

In all experiments, after extensive washing, the cells were investigated by using fluorescence microscopy. The nuclei were stained using DAPI. Samples were analysed using an Olympus BX-60 fluorescence microscope. Images were imported into Adobe Photoshop CS3 and Corel Paint Shop Pro Photo X2 for evaluation of the fluorescence intensity.

Statistical analysis

Each experiment was performed at least three times. Results are expressed as means value ± standard error of the mean (SEM). Statistical analysis was performed using unpaired Student's *t*-test using X-Plot v. 2.81 and statistical significance is expressed as * or $^\#$ $p < 0.05$ vs NG or HG group, respectively.

Results and discussion

Several studies point to neuronal cell death involvement in diabetes [32]. Contrary to these findings, we did not observe any significant viability reduction in cells exposed up to 10-fold glucose concentration (Table I). The cells incubated with HG displayed generally green intact nuclei with a very low incidence of nuclear fragmentations, suggesting prevalence of viable cells. Likewise, HG treated cells showed negligibly elevated LDH activity (110.2 ± 1.9% of control) and unaffected trypan blue viability

Table I. Quantification of viability, proliferation and morphological changes of HT22 cells exposed to high glucose.

	NG	HG
LDH activity (% of control)[a]	100 ± 1.7	110.2 ± 1.0$^\#$
Total cell number (^ 10^6)[d]	3.77 ± 0.66	1.29 ± 0.01$^\#$
Trypan blue viability (%)[b]	96.6 ± 1.5	97.3 ± 2.3
MTT reduction (% of control)[c]	100 ± 6.4	23.7 ± 0.9$^{\#\#}$
Cell cross-section area (pixel^2)[e]	2794 ± 61	7551 ± 536$^{\#\#\#}$
Perimeter (pixel)[h]	221 ± 4	395 ± 13$^{\#\#\#}$
Nuclear cross-section area (pixel^2)[f]	1074 ± 28	1669 ± 118$^{\#\#}$
Cytosolic cross-section area (pixel^2)[g]	1721 ± 40	5882 ± 417$^{\#\#\#}$
Nucleus/total cell area (%)	38.4 ± 0.6	22.1 ± 0.8$^\#$
Protein content (mg/10^6 cells)	0.11 ± 0.01	0.18 ± 0.01$^\#$

[a]Cell viability was assessed by LDH release, [b]the trypan blue exclusion test and [c]MTT reduction assay. [d]Cell number was measured by counting. Results are the means ± SEM of at least three independent determinations, $^\#p < 0.05$ $^{\#\#}p < 0.01$; vs normal glucose. The results of the cellular cross-section areas [e–g]and mean cellular perimeter [h]were calculated from the number of pixels in the selected areas by the program Adobe Photoshop CS3. The values are the mean ± SEM of at least 100 cells stained with ethidium bromide/acridine orange, $^\#p < 0.05$ $^{\#\#}p < 0.01$; vs NG. Images of the cells stained by ethidium bromide/acridine orange were captured at 48 h after incubation in NG and HG conditions using fluorescent microscope (200 × magnification).

(Table I). On the other hand, HG caused a remarkable diminution of cell proliferation and a suppression of formazan production. This is supported by the available data reporting a reduction of cell proliferation in the hippocampus (associated with disorders of cognitive abilities) of diabetic animals [33].

As further clearly shown in the fluorescent images, the high glucose led to a notable enlargement of the cells, which was also verified by the area and perimeter (Figure 1A, Table I). Thus, HG treated cells showed 2.7-fold increase of the cellular cross-section area compared to the cells exposed to normal glucose medium. Furthermore, the nuclear part was enlarged to a lesser extent compared to cytosol (Table I). Interestingly, a number of reports demonstrated morphologic abnormalities of neocortical and hypothalamic neurons in clinical studies and animal models of diabetes [34]. Concerning hippocampal tissue, reduction of the number of apical branch points as well as of the total length of apical dendrites of CA3 pyramidal neurons was shown in experimental diabetes [8]. These changes were ascribed to processes of adaptation to environmental demands termed as 'allostatic load', created by STZ-induced diabetes. In correspondence with our findings, an increased cell area of hippocampal astrocytes was reported in animal models of diabetes [35,36]. These changes were associated with an increase in the number of cells positive for GFAP (glial fibrillary acidic protein), the most common manifestation of glial hyperactivity closely related to an oxidative and hyperosmotic environment. Additionally, the presence of the polyol pathway in animal nerve and lenses and of sorbitol involved in the development of neuropathy may contribute to cell enlargement through osmotic processes [37,38]. In diabetic conditions, the accumulation of non-diffusible sorbitol creates a hyperosmotic state leading to cell swelling and increased permeability to cations, sodium and potassium. With regard to these reports, the cell swelling in our HG model suggests that the intracellular solute concentration could be still higher than that in the extracellular environment, thus diminishing the probability of a hypertonic effect of the medium in HG cells.

Furthermore, mitosis was apparently lacking in cells with increased dimension in HG treated culture. Interestingly, a limited proliferation has been found in mesangial cells exposed to high glucose, followed by cell cycle arrest in the G_1 phase and persistent and progressive hypertrophy through the mechanism involving cyclin-dependent kinase inhibitors [39]. Cellular hypertrophy has been associated with stimulated protein synthesis, increases in extracellular matrix and cellular enlargement by additional osmotic changes [40,41]. Moreover, HNE, a peroxidation product of omega-6-polyunsaturated fatty acids associated with hyperglycaemia-induced oxidative stress [9,22], was shown to induce cell cycle arrest of growing yeast [42]. Its activity as a growth regulating factor was demonstrated also in other cellular models [43–45].

Further, cell swelling was shown to act like an anabolic signal in the liver with respect to protein and carbohydrate metabolism [46].

AGEs were proposed to play an important role in secondary diabetic complications caused by

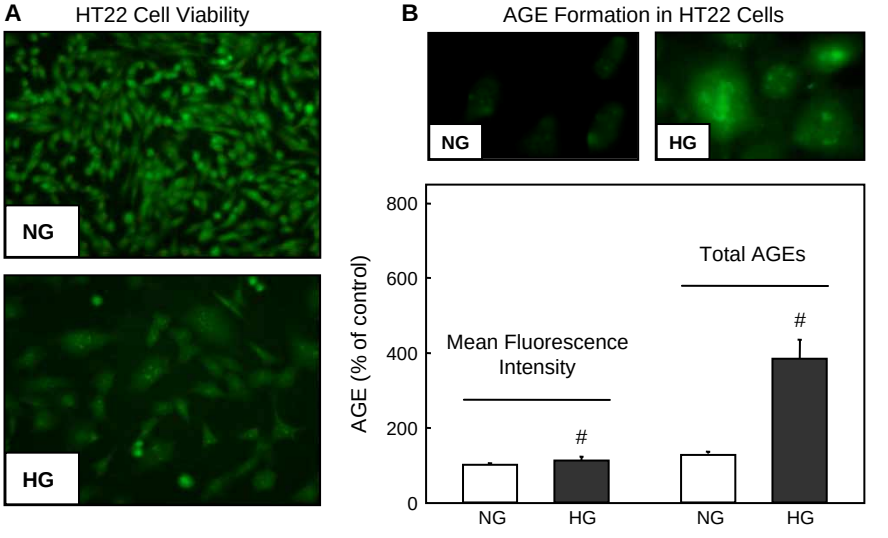

Figure 1. Cell morphology and AGE-formation in HT22 cells treated with high glucose. Images of the cells stained by ethidium bromide/acridine orange were captured at 48 h after incubation in NG or HG medium using fluorescent microscope (200×) (A). In the HT22 cells incubated in NG or HG medium AGE-modified proteins were stained and a quantitative analysis of immunofluorescence pictures was performed (B, 400×). The measured 'Mean fluorescence intensity' is shown and the calculated 'Total AGEs'. The 'Total AGEs' taking into account the increased cell volume. For calculation procedure see the main text. Results are the means ± SEM of at least 30 immunostained cells, $^{\#}p < 0.05$ vs NG. (NG = normal glucose, HG = high glucose).

hyperglycaemia [20,21,47]. As apparent from Figure 1B, a small but significant increase of AGEs immunostaining intensity was observed in the cells exposed to 48-h hyperglycaemic conditions ('mean fluorescence intensity'). On taking into account the 'dilution' of the fluorescence signal by the dramatic swelling of the cells, the enhanced formation of AGEs is clearly much more pronounced ('Total AGEs'). In general, rapid cell hypertrophy may be a cause of drop of the intracellular concentration of immunolabelled proteins resulting in reduction of the fluorescence intensity per square/pixel. When applying the quantitative equation for fluorescence radiant flux (ϕ) to the cellular compartment (1)

$$\phi = k * \zeta * \phi_0 * 2,3 * \varepsilon * l * c, \quad (1)$$

where k is the equipment constant, ϕ_0 is the fluorescence flux of the excitation light, ε is the absorption, ζ fluorescence quantum yield, l is the length of solution layer and c is the concentration of the fluorophore, the molarity ratio for fluorophores conjugated to antibodies bound to antigen in high and normal glucose cells (n_{HG} and n_{NG}, respectively) can be expressed as follows (2):

$$\begin{aligned}(n_{HG}/n_{NG}) * 100\% \\ = (V_{HG}/l_{HG}) * (l_{NG}/V_{NG}) * (\phi_{HG}/\phi_{NG}) * (\zeta_{NG}/\zeta n_{HG}) \\ =\sim \mathrm{Area}_{HG}/\mathrm{Area}_{NG} * (\phi_{HG}/\phi_{NG}) * (\zeta_{NG}/\zeta_{HG})\end{aligned} \quad (2)$$

where indexes HG and NG stand for high and normal glucose cells, V is the cellular volume and area is the dimension of cross-section area. If considering $(\zeta_{NG}/\zeta_{HG}) = 1$, there was an increase of AGEs content by $383.1 \pm 49.7\%$ of control in HG treated cells (Figure 1B). However, the less concentrated optical environment in swollen cells may lower the ratio $\zeta_{NG}/\zeta_{HG} < 1$, thus accounting for the relatively high SEM of the result.

Few data report on protein oxidation in hippocampal tissue due to high glucose conditions. Parihar et al. [48] showed a significant increase in protein carbonyls in the hippocampus of streptozotocin diabetic mice. Using immunofluorescence, only moderate rises in protein carbonyls could be seen in the nucleus (Figure 2A and B, PC/IF). Furthermore, when using equation (2) for quantitative analysis of immunofluorescence pictures (Figure 2B, 'Total PC/IF'), an increase of protein carbonyls could be demonstrated in the nuclear and cytosolic compartment. In analogy, in our high-glucose model, the protein carbonyl amount per milligram of total cellular proteins of HG cells, as measured by ELISA (Figure 2B, PC/ELISA), was similar to that of control cells (Figure 2C). The increased protein synthesis (as proved by the rise of total proteins, Table I) could however 'dilute' the accumulation of protein carbonyls. Hence, we expressed the protein carbonyls per protein content in normal glucose cells yielding the increase of absolute mass of oxidized proteins to $190.6 \pm 9.92\%$ in the cells exposed to HG (Figure 2B, 'Total PC/ELISA'). Yet again, the discrepancy with respect to the immunofluorescence result may be associated with the variation of ζ_{HG}/ζ_{NG} values for the individual cells. Also, as discussed previously, a portion of protein carbonyls is arising from site-specific protein oxidation and the results of ELISA methods reflect largely soluble cytosolic proteins.

Apart from protein glycation, a range of biochemical pathways and mechanisms of action for glucose toxicity have been illustrated by Robertson and Harmon [1] in pancreatic cells. All these pathways have in common the formation of reactive oxygen species that, in excess and over time, cause chronic oxidative stress. As demonstrated by Nishikawa et al. [49], the direct glucose toxicity in neurons is especially due to increased intracellular glucose oxidation, resulting in enhanced ROS production [50,51]. In both human and experimentally diabetic rats, oxidative stress seems to play a central role in brain damage [52,53]. In line with these reports, incubation with high glucose caused a remarkable augmentation of DCF fluorescence intensity over time (Figure 2C). This is even more pronounced if related to cell swelling (Figure 2C, 'Total DCF').

Since such an accumulation of modified proteins might also be the consequence of low proteasomal activity, a proteolytic system appears to be responsible for the degradation of oxidatively modified proteins. The proteasome is a multi-sub-unit, multicatalytic complex [54,55] and exists in two major forms—20S and 26S. The 20S proteasome is the catalytic core [56], whereas the 26S proteasome is formed by complexing of the 20S core proteasome with two 19S regulators, which have sub-units for ATP hydrolysis and polyubiquitin recognition [55]. The 20S 'core' proteasome was shown to play a key role in the degradation of oxidized proteins in ATP-independent fashion [57–61]. As shown in Figure 3A, the cells grown in HG did not display any significant changes in 20S proteasomal activity. Since the cells are increasing in size and protein content during HG treatment, this small, not significant tendency to decline in the proteasome activity might be much more dramatic when proteasome expression is concerned. The quantitative analysis of immunofluorescence pictures (when applying the intensity and cellular dimension values to the fluorescence radiant flux equations (1,2)) yielded a significant enrichment of total proteasome in both the nuclear and cytosolic compartment in HG-treated cells, demonstrating an increase of proteasome expression in correspondence with the increasing amount of proteins. In agreement with our findings, upregulation of proteasomal activity was found to be an integral part of compensatory response induced by ER stress [62], a condition commonly triggered by hyperglycaemia [63,64].

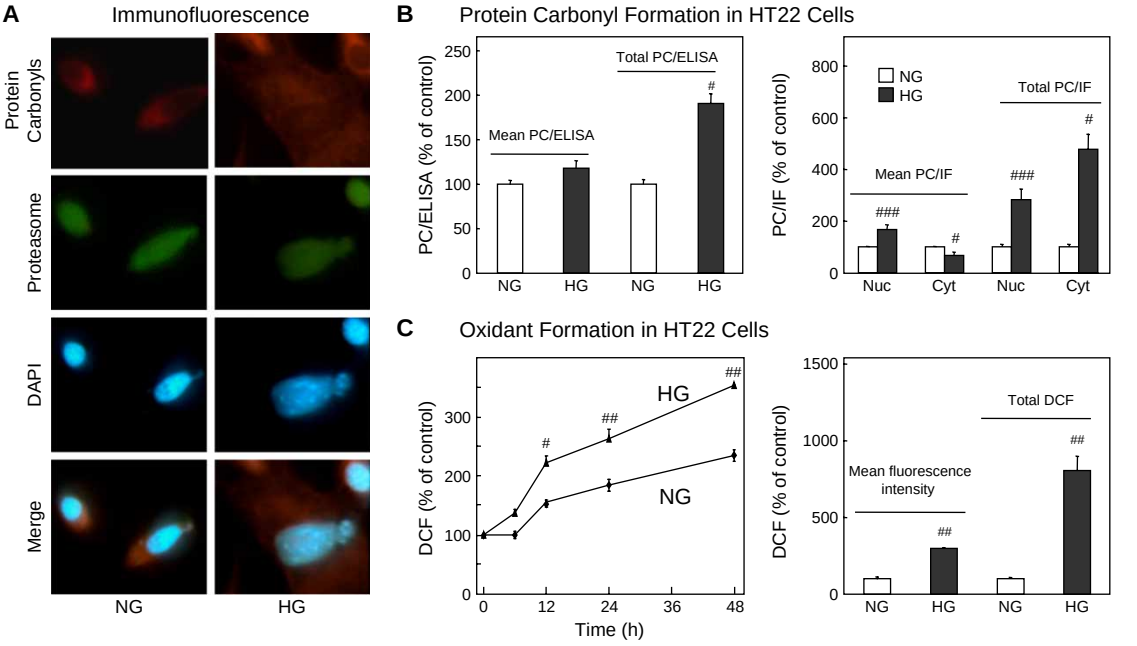

Figure 2. Oxidative protein modification and oxidant formation in HT22 cells after high glucose treatment. High glucose treated HT22 cells were immunostained for protein carbonyls, proteasome and DNA (DAPI) (A). Cells were cultured on glass bottom dishes; treatment and staining were performed as described in Methods. (B) The formation of protein carbonyls was quantified by ELISA (PC/ELISA) or quantitative immunostaining (PC/IF). The respective results are the means ± SEM of at least three independent determinations or 30 immunostained cells, $^{\#}p < 0.05$ $^{\#\#\#}p < 0.001$; vs NG. As described in the legend to Figure 1 the measured 'Mean PC' level and the calculated 'Total PC' level is shown. Immunofluorescent quantification was performed separately for the nucleus ('Nuc') and the cytosol ('Cyt'). Time-dependent oxidant production in high glucose treated HT22 cells is shown in (C) (left part). The right part of (C) demonstrates the values after 48 h, again as measured 'Mean fluorescence intensity' and calculated 'Total DCF'. For calculation procedure see the main text and legend to Figure 1. Results are the means ± of at least three independent determinations, $^{\#}p < 0.05$ $^{\#\#\#}p < 0.001$;vs NG (NG = normal glucose, HG = high glucose).

Furthermore, glycoxidative stress was shown to upregulate the nuclear proteasomal activity. This upregulation was achieved by both increased proteasomal activity and increased number of proteasomes [65].

Our previous work demonstrated alterations of intracellular distribution of oxidized proteins, proteasome and proteins in HT22 cells following exposure to various oxidants. As outlined by Keller [66], the well-organized interplay between protein synthesis, protein degradation and protein oxidation is likely to prevent the development of lethal oxidative stress. Accordingly, the increased turnover of proteins in HT22 cells, due to HG exposure associated with a boost of protein synthesis and acceleration of protein degradation, may be responsible for the non-lethal

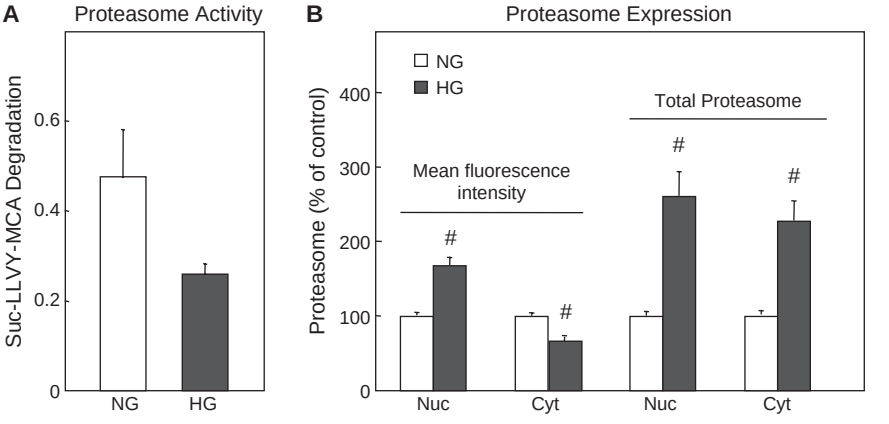

Figure 3. Proteasome activity and expression in high glucose treated HT22 cells. The ATP-independent (20S proteasome) activity was assessed by cleavage of the fluorogenic substrate suc-LLVY-AMC and quantification of free AMC by spectrofluorometric measurements (A). Quantitative analysis of immunofluorescence of the HT22 cells stained for proteasome using polyclonal anti-proteasome antibody is shown in (B). As stated above 'Mean fluorescence intensity' is the measured value, whereas 'Total proteasome' is a calculated value taking into account cell swelling (see text). The analysis was performed for the nuclear ('Nuc') and cytosolic ('Cyt') region of cells. Results are the means ± SEM of at least three independent determinations or at least 30 immunostained cells, $^{\#}p < 0.05$ vs NG.

carbonyl concentration in proteins. Conversely, apart from the increased protein synthesis, a decreased protein degradation through a decline of the activity of cathepsins B and L have been proposed to be a cause of the renal protein mass increases observed in diabetic renal hypertrophy and enlargement of the mesangial cells exposed to HG [39,41]. This could put emphasis on the proteasome as an early defense system for the clearance of oxidized proteins, thus preventing non-degradable material accumulation with potentially lethal effects to the neuronal cells exposed to hyperglycaemia.

Different pathways have been described within glucose metabolism in pancreatic islets through which high concentrations of glucose can lead to the accumulation of reactive oxygen species [1]. This includes the non-enzymatic glycoxidation pathways and the metabolism of glucose leading to an enhanced energy production and mitochondrial activity. In order to discriminate between these possibilities, we used the non-metabolizable glucose analogue 2-deoxy-D-glucose, also able to react in non-enzymatic glycoxidation pathways, citrate as an inhibitor of the early glucose metabolism via the phosphofructokinase and finally a potential antioxidant as a control for the role of reactive species in the induced metabolic changes (±)-cis-8-methoxy- 1,3,4,4a,5,9b -hexahydro-pyrido[4,3-b]indole-2-carboxylic acid ethyl ester. 2-deoxy-D-glucose (dG), a non-metabolizable glucose analogue [67,68], was shown to protect hippocampal neurons against excitotoxic injury [69] in a manner associated with decreasing levels of cellular oxidative stress. Correspondingly, citrate (Cit), a Krebs cycle intermediate that inhibits the activity phosphofructokinase [70], was shown to protect neuronal cells under hypoxic conditions through modulation of glucose metabolism [71]. Ultimately, we assessed the protective effects of (±)-cis-8-methoxy-1,3,4,4a,5,9b-hexahydro-pyrido [4,3-b]indole-2-carboxylic acid ethyl ester (AO) [23,24], a derivative of the hexahydropyridoindole drug stobadine, an efficient chain-breaking antioxidant [72], showing protective effects in a variety of tissues in animal models of diabetes [73–75].

Interestingly, all three substances used reduced significantly cell swelling as measured by cell perimeter and cell area (Figure 4A). The increase of protein synthesis due to high glucose has been described in various cellular models [76–78]. In addition, in line with the proposed relationship between cell swelling and stimulation of protein synthesis [46], the cell area parameter appeared to correlate to some extent with the protein content increase in high glucose cells and HG cells treated with AO and citrate. In addition, apart from the lack of cell enlargement, the high-deoxyglucose (HdG) treated cells did slightly shrink, which may point to hypertonic effect of the fluid environment (3.5% dG). Thus, this outcome underscores the role of increased intracellular tonicity in swelling HG cells (probably, due to enhanced accumulation of glucose metabolites [37,38]), rather than a hypertonic effect of the concentrated environment. Citrate and AO improved the reduced cell proliferation and viability (Figure 4 B and C). Citrate was established also as an aldose reductase inhibitor (an uncompetitive inhibitor in the forward reaction with respect to aldehyde reduction), while it is a competitive inhibitor with respect to alcohol in the backward reaction (oxidation of alcohol)) [79]. On the other hand, HdG rather reduced the cell number and had a more dramatic effect on cell viability in comparison to HG treatment, most likely due to the lack of energy in the cells (Figure 4 B and C). Pre-treatment of rat hippocampal cell cultures with 2-deoxy-D-glucose decreased the vulnerability of neurons to excitotoxic and oxidative

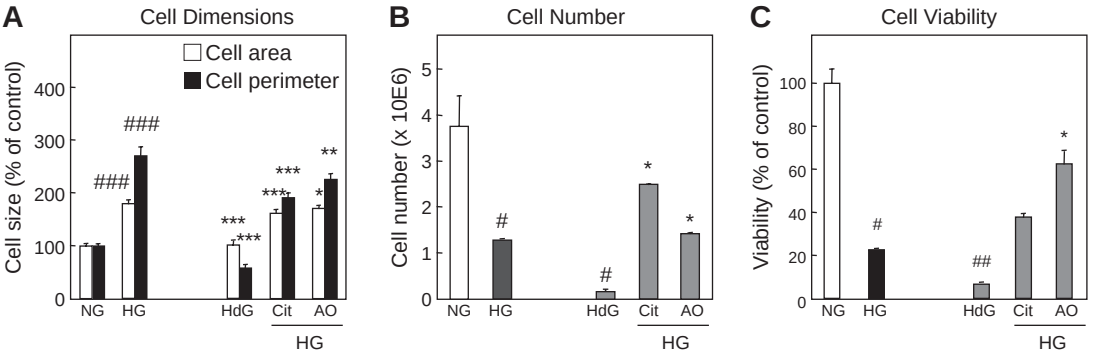

Figure 4. Effect of inhibitors on cell morphology and viability in HT22 cells treated with high glucose. Effects of glycolysis inhibitors on cell morphology (A), proliferation (B) and viability (C) in control cells (NG) or HT22 cells incubated with high glucose (HG) or high deoxyglucose (HdG). The results of the cellular cross-section areas and mean cellular perimeter (A) were calculated from the number of pixels in the selected areas by the program Adobe Photoshop CS3. Viable cells were counted after trypan blue exclusion (B) and the MTT test was further used as a viability test (C). (Cit = citrate, AO = (±)-8-methoxy-1,3,4,4a,5,9b-hexahydro-pyrido[4,3-b]indole-2-carboxylic acid ethyl ester). The values are the means ± SEM of least 100 cells stained with ethidium bromide/acridine orange (A) or three independent determinations (B and C), $^{\#}p<0.05$ $^{\#\#}p<0.01$, $^{\#\#\#}p<0.001$ or $^{*}p<0.05$ $^{**}p<0.01$, $^{***}p<0.001$ vs NG or HG group, respectively.

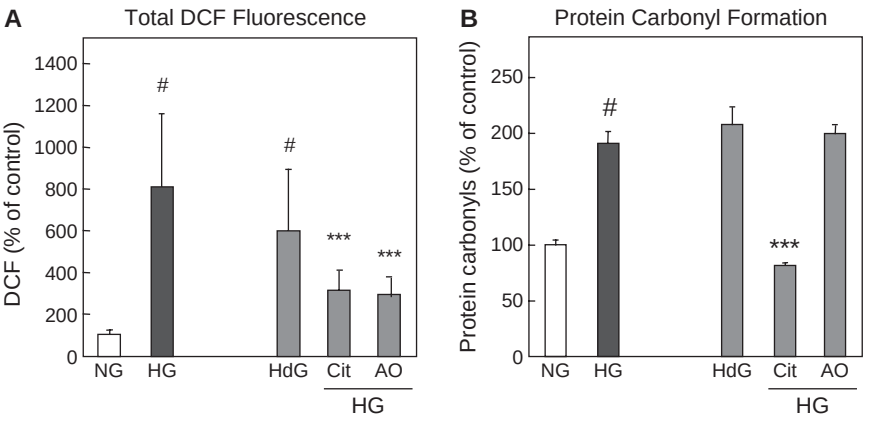

Figure 5. Effect of inhibitors on oxidative protein modification and oxidant formation in HT22 cells after high glucose treatment. Effects of glycolysis inhibitors on oxidant production (A) and protein carbonyl formation (B) in control cells (NG) or HT22 cells incubated with high glucose (HG) or high deoxyglucose (HdG). Protein carbonyl content was measured by ELISA. Cit = citrate, AO = (±)-8-methoxy-1,3,4,4a,5,9b-hexahydro-pyrido[4,3-b]indole-2-carboxylic acid ethyl ester. Results are the means ± SEM of at least three independent determinations, $^{\#}p < 0.05$ or $^{*}p < 0.05$ $^{***}p < 0.001$ vs NG or HG group, respectively.

insults [69]. On the contrary, glycolytic flux restriction in HT22 cells was found to have a lethal effect [80]. Moreover, the induction of oxidative stress was documented during glucose starvation or hypoglycaemia *in vivo* or in cell culture models [81–83]. Nevertheless, hyperosmotic stress (assumably induced in HdG cells) was reported to increase ROS and protein carbonylation *in vitro* and *in vivo* [84,85]. This was confirmed in our model showing high H_2DCF and high protein oxidation in cells incubated in high-deoxyglucose (Figure 5 A and B). However, citrate and AO suppressed the intracellular generation of ROS as measured by DCF fluorescence. Interestingly, AO was not able to suppress protein carbonyl formation. This could be an effect of non-oxidative introduction of carbonyl groups into the protein pool, simply by chemical modification with glucose. This process will not be suppressed by an antioxidant and, therefore, a reduction of DCF fluorescence and high protein carbonyl levels can be expected.

These results point to a role of the processes downstream of the glucose entry and ingress to its metabolism in the ROS production in neuronal tissue exposed to hyperglycaemia [1]. Thus, our results highlight the role of oxidative stress in the toxic effect of glucose to neuronal cells in diabetes. High glucose, through enhanced glucose metabolism followed by over-production of ROS, can trigger harmful effects to the neuronal cells. Our findings may have future potential clinical consequences as they provide better understanding of factors which may protect neurons from injury caused by oxidative stress during hyperglycaemia.

Acknowledgements

This work was supported by COST Action B35 Lipid Peroxidation Associated Disorders: LPO, APVV-51-017905 and VEGA 2/0086/08.

***Declaration of interest*:** The authors report no conflicts of interest. The authors alone are responsible for the content and writing of the paper.

References

[1] Robertson RP, Harmon JS. Diabetes, glucose toxicity, and oxidative stress: a case of double jeopardy for the pancreatic islet beta cell. Free Radic Biol Med 2006;41:177–184.
[2] Brown MJ, Asbury AK. Diabetic neuropathy. Ann Neurol 1983;15:2–12.
[3] Niakan E, Harati Y, Comstock JP. Diabetic autonomic neuropathy. Metabolism 1986;35:224–234.
[4] McCall AL. The impact of diabetes on the CNS. Diabetes 1992;41:557–570.
[5] Biessels G-J, Kappelle AC, Bravenboer B, Erkelens DW, Gispen WH. Cerebral function in diabetes mellitus. Diabetologia 1994;37:643–650.
[6] Bestetti G, Locatelli V, Tirone F, Rossi GL, Muller EE. One month of streptozotocin-diabetes induces different neuroendocrine and morphological alterations in the pituitary axis of male and female rats. Endocrinology 1985;117:208–216.
[7] Bestetti G, Rossi GL. Hypothalamic changes in diabetic Chinese hamsters. Lab Invest 1982;47:516–522.
[8] Magariños AM, McEwen BS. Experimental diabetes in rats causes hippocampal dendritic and synaptic reorganization and increased glucocorticoid reactivity to stress. Proc Natl Acad Sci USA 2000;97:11056–11061.
[9] Reagan LP. Glucose, stress and hippocampal neuronal vulnerability. Int Rev Neurobiol 2002;51:289–324.
[10] Tay SSW, Wong WC. Gracile nucleus of streptozotocin-induced diabetic rats. J Neurocytol 1991;20:356–364.

[11] Flood JF, Mooradian AD, Morley JE. Characteristics of learning and memory in streptozocin-induced diabetic mice. Diabetes 1990;39:1391–1398.
[12] De Nicola AF, Magariños AM, Foglia VG. Neuroendocrine regulation in experimental diabetes (Houssay Lecture). In: H Rifkin, JA Colwell, SI Taylor, editors. Diabetes. Amsterdam: Elsevier; 1991. p 3–8.
[13] De Nicola AF, Magariños AM, Foglia VG. Neuroendocrine regulation in experimental diabetes (Houssay Lecture). In: H Rifkin, JA Colwell, SI Taylor, editors. Diabetes. Amsterdam: Elsevier; 1991. p 3–8.
[14] Chabot CH, Massicotte G, Milot M, Trudeau F, Gagne J. Impaired modulation of AMPA receptors by calcium-dependent processes in streptozotocin-induced diabetic rats. Brain Res 1997;768:249–256.
[15] Baynes JW, Thorpe SR. Role of oxidative stress in diabetic complications: a new perspective on an old paradigm. Diabetes 1999;48:1–9.
[16] Greene DA, Stevens MJ, Obrosova I, Feldman EL. Glucose-induced oxidative stress and programmed cell death in diabetic neuropathy. Eur J Pharmacol 1999;375:217–223.
[17] Lovell MA, Ehmann WD, Butler SM, Markesbery WR. Elevated thiobarbituric acid-reactive substances and antioxidant enzyme activity in the brain in Alzheimer's disease. Neurology 1995;45:1594–1601.
[18] Aragno M, Mastrocola R, Brignardello E, Catalano M, Robino G, Manti R, Parola M, Danni O, Boccuzzi G. Dehydroepiandrosterone modulates nuclear factor-kappaB activation in hippocampus of diabetic rats. Endocrinology 2002;143:3250–3258.
[19] Grillo CA, Piroli GG, Rosell DR, Hoskin EK, Mcewen BS, Reagan LP. Region specific increases in oxidative stress and superoxide dismutase in the hippocampus of diabetic rats subjected to stress. Neuroscience 2003;121:133–140.
[20] Wolff SP, Dean RT. Glucose autoxidation and protein modification: the potential role of autoxidative glycosylation in diabetes. Biochem J 1987;245:243–250.
[21] Simpson JA, Narita S, Gieseg S, Gebicki S, Gebicki JM, Dean RT. Long-lived reactive species on free-radical-damaged proteins. Biochem J 1992;282:621–624.
[22] Reagan LP, Magarinos AM, Yee DK, Swzeda LI, Van Bueren A, McCall A, McEwen BS. Oxidative stress and HNE conjugation of GLUT3 are increased in the 1 hippocampus of diabetic rats subjected to stress. Brain Res 2000;862:292–300.
[23] Stolc S, Bauer V, Benes L, Tichy M. Medicine with antiarrhythmic and antihypoxic activity and its methods of preparation. Patent CS 229067, SWED 8204693–9, BELG 894148, SWISS 651 754, BRD P-323 1088, SPAIN 553 017 JAP 1983;151:4040.
[24] Stolc S, Povazanec F, Bauer V, Majekova M, Wilcox AL, Snirc V, Rackova L, Sotnikova R, Stefek M, Gasparova-Kvaltinova Z, Gajdosikova A, Mihalova D. Slovak Patent Registration PP 1321. 2003.
[25] Tolnai S. A method for viable cell count. Methods Cell Sci 1975;1:37–38.
[26] Ribble D, Goldstein NB, Norris DA, Shellman YG. A simple technique for quantifying apoptosis in 96-well plates. BMC Biotechnol 2005;5:12–19.
[27] Giardina C, Inan MS. Nonsteroidal anti-inflammatory drugs, short-chain fatty acids, and reactive oxygen metabolism in human colorectal cancer cells. Biochim Biophys Acta 1998;1401:277–288.
[28] Swift LM, Sarvazyan N. Localization of dichlorofluorescin in cardiac myocytes: implications for assessment of oxidative stress. Am J Physiol Heart Circ Physiol 2000;278:H982–H990.
[29] Buss H, Chan TP, Sluis KB, Domigan NM, Winterbourn CC. Protein carbonyl measurement by a sensitive ELISA method. Free Radic Biol Med 1997;23:361–366.
[30] Jung T, Engels M, Kaiser B, Poppek D, Grune T. Intracellular distribution of oxidized proteins and proteasome in HT22 cells during oxidative stress. Free Radic Biol Med 2006;40:1303–1312.
[31] Smith MA, Syre LM, Anderson VE, Harris PLR, Beal MF, Kowall N, Perry G. Cytochemical demonstration of oxidative damage in Alzheimer disease by immunochemical enhancement of the carbonyl reaction with 2,4-dinitrophenylhydrazine. J Histochem Cytochem 1998;46:731–735.
[32] Li ZG, Zhang W, Grunberger G, Sima AA. Hippocampal neuronal apoptosis in type 1 diabetes. Brain Res 2002;946:221–231.
[33] Jackson-Guilford J, Leander JD, Nisenbaum LK. The effect of streptozotocin-induced diabetes on cell proliferation in the rat dentate gyrus. Neurosci Lett 2000;293:91–94.
[34] Reagan LP, Magarinos AM, McEwen BS. Neurological changes induced by stress in streptozotocin diabetic rats. Ann NY Acad Sci 1999;893:126–137.
[35] Saravia FE, Revsin Y, Deniselle MCG, Gonzalez SL, Roig P, Lima A, Homo-Delarche F, De Nicola AF. Increased astrocyte reactivity in the hippocampus of murine models of type 1 diabetes: the nonobese diabetic (NOD) and streptozotocin-treated mice. Brain Res 2002;957:345–353.
[36] Baydas G, Reiter RJ, Yasar A, Tuzcu M, Akdemir I, Nedzvetskij VS. Melatonin reduces glial reactivity in the hippocampus, cortex, and cerebellum of streptozotocin-induced diabetic rats. Free Radic Biol Med 2003;35:797–804.
[37] Kinoshita JH, Kador P, Catiles M. Aldose reductase in diabetic cataracts. JAMA 1981;246:246–257.
[38] Greene DA, Sima AAF, Stevens MJ, Feldman EL, Lattimer SA. Complications: neuropathy, pathogenetic considerations. Diabetes Care 1992;15:1902–1925.
[39] Wolf G, Schroeder R, Zahner G, Stahl RAK, Shankland SJ. High glucose-induced hypertrophy of mesangial cells requires p27Kip1, an inhibitor of cyclin-dependent kinases. Am J Pathol 2001;158:1091–1100.
[40] Wolf G, Thaiss F. Hyperglycaemia—pathophysiological aspects at the cellular level. Nephrol Dial Transplant 1995;10:1109–1112.
[41] Olbricht CJ, Geissinger B. Renal hypertrophy in streptozotocin diabetic rats: role of proteolytic lysosomal enzymes. Kidney Int 1992;11:966–972.
[42] Wonisch W, Kohlwein SD, Schaur J, Tatzber F, Guttenberger H, Zarkovic N, Winkler R, Esterbauer H. Treatment of the budding yeast Saccharomyces cerevisiae with the lipid peroxidation product 4-HNE provokes a temporary cell cycle arrest in G1 phase. Free Radic Biol Med 1998;25:682–687.
[43] Poljak-Blazi M, Zarkovic N, Schaur RJ. Impaired proliferation and DNA synthesis of a human tumor cell line (HeLa) caused by short treatment with the anti-anemic drug jectofer (ferric-sorbitol-citrate) and the lipid peroxidation product 4-hydroxynonenal. Cancer Biother Radiopharm 1998;13:395–401.
[44] Kreuzer T, Grube R, Wutte A, Zarkovic N, Schaur RJ. 4-Hydroxynonenal modifies the effects of serum growth factors on the expression of the c-fos proto-oncogene and the proliferation of HeLa carcinoma cells. Free Radic Biol Med 1998;25:42–49.
[45] Kreuzer T, Zarković N, Grube R, Schaur RJ. Inhibition of HeLa cell proliferation by 4-hydroxynonenal is associated with enhanced expression of the c-fos oncogene. Cancer Biother Radiopharm 1997;12:131–136.
[46] Häussinger D. The role of cellular hydration in the regulation of cell function. Biochem J 1996;313:697–710.

[47] Gieseg SP, Simpson JA, Charlton TS, Duncan MW, Dean RT. Protein-bound 3,4-dihydroxyphenylalanine is a major reductant formed during hydroxyl radical damage to proteins. Biochemistry 1993;32:4780–4786.
[48] Parihar MS, Chaudhary M, Shetty R, Hemnani T. Susceptibility of hippocampus and cerebral cortex to oxidative damage in streptozotocin treated mice: prevention by extracts of Withania somnifera and Aloe vera. J Clin Neurosci 2004;11:397–402.
[49] Nishikawa T, Edelstein D, Du XL, Yamagishi S, Matsumura T, Kaneda Y, Yorek MA, Beebe D, Oates PJ, Hammes HP, Giardino I, Brownlee M. Normalizing mitochondrial superoxide production blocks three pathways of hyperglycaemic damage. Nature 2000;404:787–790.
[50] Bonnefont-Rousselot D. Glucose and reactive oxygen species. Curr Opin Clin Nutr Metab Care 2002;5:561–568.
[51] Evans JL, Goldfine ID, Maddux BA, Grodsky GM. Oxidative stress and stress-activated signaling pathways: a unifying hypothesis of type 2 diabetes. Endocrine Rev 2002;23:599–622.
[52] Aragno M, Parola S, Brignardello E, Mauro A, Tamagno E, Manti R, Danni O, Boccuzzi G. Dehydroepiandrosterone prevents oxidative injury induced by transient ischemia/reperfusion in the brain of diabetic rats. Diabetes 2000;49:1924–1931.
[53] Aragno M, Parola S, Tamagno E, Brignardello E, Manti R, Danni O, Boccuzzi G. Oxidative derangement in rat synaptosomes induced by hyperglycaemia: restorative effect of dehydroepiandrosterone treatment. Biochem Pharmacol 2000;60:389–395.
[54] Jung T, Bader N, Grune T. Oxidized proteins: Intracellular distribution and recognition by the proteasome. Arch Biochem Biophys 2007;462:231–237.
[55] Levine RL, Garland D, Oliver CN, Amici A, Climent I, Lenz AG, Ahn BW, Shaltiel S, Stadtman ER. Determination of carbonyl content in oxidatively modified proteins. Methods Enzymol 1990;186:464–478.
[56] Coux O, Tanaka K, Goldberg AL. Structure and functions of the 20S and 26S proteasomes. Annu Rev Biochem 1996;29:10289–10297.
[57] Rivett AJ. Proteasomes: multicatalytic proteinase complexes. Biochem J 1993;291:1–10.
[58] Stroh A, Zimmer C, Gutzeit C, Jakstadt M, Marschinke F, Jung T, Pilgrimm H, Grune T. Iron-oxide-particles for molecular magnetic resonance-imaging cause transient oxidative stress in rat macrophages. Free Radic Biol Med 2004;36:976–984.
[59] Mehlhase J, Sandig G, Pantopoulos K, Grune T. Oxidation-induced ferritin turnover in microglial cells: role of proteasome. Free Radic Biol Med 2005;38:276–285.
[60] Petropoulos I, Friguet B. Protein maintenance in aging and replicative senescence: a role for the peptide methionine sulfoxide reductase. Biochim Biophys Acta 2005;1703:261–266.
[61] Dunlop RA, Rodgers KJ, Dean RT. Recent developments in the intracellular degradation of oxidized proteins. Free Radic Biol Med 2002;33:894–906.
[62] Cullinan SB, Diehl JA. Coordination of ER and oxidative stress signaling: the PERK/Nrf2 signaling pathway. Int J Biochem Cell Biol 2006;38:317–332.
[63] Unger RH. Lipotoxic diseases. Annu Rev Med 2002;53:319–336.
[64] Wang H, Kouri G, Wollheim CB. ER stress and SREBP-1 activation are implicated in beta-cell glucolipotoxicity. J Cell Sci 2005;118:3905–3915.
[65] Cervantes-Laurean D, Roberts MJ, Jacobson EL, Jacobson MK. Nuclear proteasome activation and degradation of carboxymethylated histones in human keratinocytes following glyoxal treatment. Free Radic Biol Med 2005;38:786–795.
[66] Keller JN. Interplay between oxidative damage, protein synthesis, and protein degradation in Alzheimer's disease. J Biomed Biotechnol 2006;2006:1–3.
[67] German SM. Glucose sensing in pancreatic islet beta cells: the key role of glucokinase and the glycolytic intermediates. Proc Natl Acad Sci USA 1993;90:1781–1785.
[68] Salas J, Salas M, Viruela E, Sols A. Glucokinase of rabbit liver. Purification properties. J Biol Chem 1965;240:1014–1018.
[69] Lee J, Bruce-Keller AJ, Kruman Y, Chan SL, Mattson MP. 2-deoxy-d-glucose protects hippocampal neurons against excitotoxic and oxidative injury: evidence for the involvement of stress proteins. J Neurosci Res 1999;57:48–61.
[70] Staal GE, Kalff A, Heesbeen EC, Van Veelen CWM, Rijksen G. Subunit composition, regulatory properties, and phosphorylation of phosphofructokinase from human gliomas. Cancer Res 1987;47:5047–5051.
[71] Kelleher JA, Chan TYY, Chan PH, Gregory GA. Protection of astrocytes by fructose 1,6-bisphosphate and citrate ameliorates neuronal injury under hypoxic conditions. Brain Res 1996;726:167–173.
[72] Horakova L, Stolc S. Antioxidant and pharmacodynamic effects of pyridoindole stobadine. Gen Pharmacol 1998;30:627–638.
[73] Stefek M, Sotnikova R, Okruhlicova L, Volkovova K, Kucharska J, Gajdosik A, Gajdosikova A, Mihalova D, Hozova R, Tribulova N, Gvozdjakova A. Effect of dietary supplementation with the pyridoindole antioxidant stobadine on antioxidant state and ultrastructure of diabetic rat myocardium. Acta Diabetol 2000;37:111–117.
[74] Stefek M, Gajdosik A, Tribulova N, Navarova J, Volkovova K, Weismann P, Gajdosikova A, Drimal J, Mihalova D. The pyridoindole antioxidant stobadine attenuates albuminuria, enzymuria, kidney lipid peroxidation and matrix collagen cross-linking in streptozotocin-induced diabetic rats. Methods Find Exp Clin Pharmacol 2002;24:565–571.
[75] Ulusu NN, Sahilli M, Avci A, Canbolat O, Ozansoy G, Ari N, Bali M, Stefek M, Stolc S, Gajdosik A, Karasu C. Pentose phosphate pathway, glutathione-dependent enzymes and antioxidant defense during oxidative stress in diabetic rodent brain and peripheral organs: effects of stobadine and vitamin E. Neurochem Res 2003;28:815–823.
[76] Tokudome T, Horio T, Yoshihara F, Suga S, Kawano Y, Kohno M, Kangawa K. Direct effects of high glucose and insulin on protein synthesis in cultured cardiac myocytes and DNA and collagen synthesis in cardiac fibroblasts. Metabolism 2004;53:710–715.
[77] Gomez E, Powell ML, Greenman IC, Herbert TP. Glucose-stimulated protein synthesis in pancreatic β-cells parallels an increase in the availability of the translational ternary complex (eIF2-GTP Met-tRNAi) and the dephosphorylation of eIF2α. J Biol Chem 2004;279:53937–53946.
[78] Yeshao W, Gu J, Peng X, Nairn AC, Nadler JL. Elevated glucose activates protein synthesis in cultured cardiac myocytes. Metabolism 2005;54:1453–1460.
[79] Harrison DH, Bohren KM, Ringe D, Petsko GA, Gabbay KH. An anion binding site in human aldose reductase: mechanistic implications for the binding of citrate, cacodylate, and glucose 6-phosphate. Biochemistry 1994;33:2011–2020.
[80] Sagara Y, Schubert D. The activation of metabotropic glutamate receptors protects nerve cells from oxidative stress. J Neurosci 1998;18:6662–6671.
[81] Jekabsone A, Neher JJ, Borutaite V, Brown GC. Nitric oxide from neuronal nitric oxide synthase sensitises neurons

to hypoxia-induced death via competitive inhibition of cytochrome oxidase. J Neurochem 2007;103:346–356.
[82] Ikeda J, Ma L, Morita I, Murota S. Involvement of nitric oxide and free radical (O2-) in neuronal injury induced by deprivation of oxygen and glucose *in vitro*. Acta Neurochir Suppl (Wien) 1994;60:94–97.
[83] Papadopoulos MC, Koumenis IL, Dugan LL, Giffard RG. Vulnerability to glucose deprivation injury correlates with glutathione levels in astrocytes. Brain Res 1997;748:151–156.
[84] Kultz D. Hyperosmolality triggers oxidative damage in kidney cells. Proc Natl Acad Sci USA 2004;101:9177–9178.
[85] Zhang Z, Dmitrieva NI, Park JH, Levine RL, Burg MB. High urea and NaCl carbonylate proteins in renal cells in culture and *in vivo*, and high urea causes 8-oxoguanine lesions in their DNA. Proc Natl Acad Sci USA 2004; 101:9491–9496.

This paper was first published online on iFirst on 24 July 2009.